Acta Biomaterialia 9 (2013) 7948–7956

Contents lists available at SciVerse ScienceDirect

Acta Biomaterialia

journal homepage: www.elsevier.com/locate/actabiomat

Helical sub-structures in energy-storing tendons provide a possible mechanism for efficient energy storage and return

Chavaunne T. Thorpe [a,b,*], Christian Klemt [a], Graham P. Riley [c], Helen L. Birch [d], Peter D. Clegg [b], Hazel R.C. Screen [a]

[a] Institute of Bioengineering, School of Engineering and Materials Science, Queen Mary, University of London, Mile End Road, London E1 4NS, UK
[b] Department of Musculoskeletal Biology, Institute of Ageing and Chronic Disease, University of Liverpool, Leahurst Campus, Neston CH64 7TE, UK
[c] School of Biological Sciences, University of East Anglia, Norwich Research Park, Norwich NR4 7TJ, UK
[d] Institute of Orthopaedics and Musculoskeletal Science, University College London, Stanmore HA7 4LP, UK

ARTICLE INFO

Article history:
Received 12 March 2013
Received in revised form 18 April 2013
Accepted 2 May 2013
Available online 10 May 2013

Keywords:
Fascicle
Structure–function
Micromechanics
Confocal microscopy

ABSTRACT

The predominant function of tendons is to position the limb during locomotion. Specific tendons also act as energy stores. Energy-storing (ES) tendons are prone to injury, the incidence of which increases with age. This is likely related to their function; ES tendons are exposed to higher strains and require a greater ability to recoil than positional tendons. The specialized properties of ES tendons are thought to be achieved through structural and compositional differences. However, little is known about structure–function relationships in tendons. This study uses fascicles from the equine superficial digital flexor (SDFT) and common digital extensor (CDET) as examples of ES and positional tendons. We hypothesized that extension and recoil behaviour at the micro-level would differ between tendon types, and would alter with age in the injury-prone SDFT. Supporting this, the results show that extension in the CDET is dominated by fibre sliding. By contrast, greater rotation was observed in the SDFT, suggesting a helical component to fascicles in this tendon. This was accompanied by greater recovery and less hysteresis loss in SDFT samples. In samples from aged SDFTs, the amount of rotation and the ability to recover decreased, while hysteresis loss increased. These findings indicate that fascicles in the ES SDFT may have a helical structure, enabling the more efficient recoil observed. Further, the helix structure appears to alter with ageing; this coincides with a reduction in the ability of SDFT fascicles to recoil. This may affect tendon fatigue resistance and predispose aged tendons to injury.

1. Introduction

Tendons have multiple mechanical requirements which are specific to tendon type and relate to different functional roles. Precise mechanical properties are essential for efficient function and are conferred on the tendon by a complex hierarchical structure, in which highly aligned type I collagen is grouped together, forming sub-units of increasing diameter. Triple-helical collagen molecules are cross-linked together to form fibrils, which aggregate to form fibres. The fibres combine, forming fascicles, which are the largest sub-structural unit of tendons. Each hierarchical level is interspersed with a small amount of proteoglycan-rich matrix [1]. Structural and compositional alterations throughout this hierarchy are thought to result in the distinct mechanical properties required by functionally different tendons.

Tendons can be broadly categorized by their function; while all tendons have a positional role, some also operate as energy stores to decrease the energetic cost of locomotion [2]. Positional and energy-storing (ES) tendons have differing mechanical demands. To enable efficient force transfer, positional tendons need to be relatively stiff, whereas ES tendons require a degree of compliance to maximize energy storage [3,4], and they also need to recoil rapidly to return energy to the system [5]. Further, ES tendons need to be able to withstand large extensions; strains of up to 11% and 16% have been recorded in the human Achilles tendon and equine superficial digital flexor tendon (SDFT), respectively, during maximal exercise [6,7]. This extension capacity is not required in positional tendons such as the human anterior tibialis tendon and equine common digital extensor tendon (CDET), which experience strains in the region of 2–3% during normal use [8,9]. Correspondingly, previous work has shown that failure properties differ between tendon types, with the equine SDFT failing at higher strains than the CDET when tested in vitro [10,11].

Despite this ability to withstand higher strains, energy-storing tendons have a much greater predisposition to injury than

* Corresponding author at: Institute of Bioengineering, School of Engineering and Materials Science, Queen Mary, University of London, Mile End Road, London E1 4NS, UK. Tel.: +44 20 7882 5368.
E-mail address: c.thorpe@qmul.ac.uk (C.T. Thorpe).

1742-7061/$ - see front matter © 2013 Acta Materialia Inc. Published by Elsevier Ltd. All rights reserved.
http://dx.doi.org/10.1016/j.actbio.2013.05.004

positional tendons, likely due to the extremely high strains they experience in vivo. The initiation and progression of tendon injury is similar between humans and horses [12,13]; the human Achilles is the most commonly injured tendon in runners [14], and the equine SDFT is also highly susceptible to injury, specifically localized to the tendon core in the mid-metacarpal region (for a detailed review see Thorpe et al. [15] and references therein). Further, the risk of injury increases significantly with age in both human and equine ES tendons [14,16–18]. However, it has not been fully established how the structure of functionally distinct tendons is specialized for their specific roles, and if any age-related alterations occur to the structure of ES tendons which predisposes them to injury.

Previous studies have investigated micromechanics within isolated fascicles as it is possible to remove these from tendons without damaging their structure, and they provide a complete unit that is suitable in size for microstructural analysis. Studies using this approach have established that fascicle extension occurs predominantly as a result of sliding between adjacent fibres and fibrils, with only a small amount of extension occurring within the collagen units themselves [19–26]. Recoverability has also been assessed, with the results showing that both fibre sliding and fibre extension are reversible after the application of up to 5% strain [20,24]. The majority of studies have used rat tail tendon fascicles as this provides a simple model to develop an understanding of tendon micromechanics, and few studies have assessed how mechanics vary between tendon types. However, one recent study has reported that the microstructural stress relaxation response differs between the functionally distinct porcine SDFT and CDET, resulting in more rapid stress relaxation in fascicles from the positional CDET [27].

The majority of these studies have used fluorescent dyes to visualize the cell nuclei under a confocal microscope and measured the displacement between nuclei in the same or adjacent rows to infer fibre extension and sliding. However, the relationship between the cells and their surrounding matrix will influence the observed response [28]. An alternative approach is to stain the collagen and then photobleach a grid into the dye. The deformation of the grid can then be quantified, allowing direct assessment of the matrix response to applied strain [28]. This approach has been used previously to investigate micromechanics in rat tail tendon fascicles and other collagen-rich tissues including the intervertebral disc [28,29]. These studies have ascertained that the microstructural response to applied strain is complex and heterogeneous, with fibre sliding dominating extension. However, mechanisms governing fascicle recovery after strain has been applied have not been investigated using this approach, and it has not been established if extension or recovery behaviour varies between functionally distinct tendons. Further, no studies have investigated the effect of increasing age on the microstructural strain response within tendon fascicles.

In this study, we investigated the extension and recovery mechanisms in fascicles from the high strain ES SDFT and low strain positional CDET from young and old horses. We hypothesized that the extension and recoil mechanisms would differ in fascicles from the equine SDFT and CDET, resulting in more efficient recoil in SDFT samples. We further hypothesized that ageing would result in altered extension mechanisms and less efficiency of recoil in SDFT fascicles, whereas the response of CDET fascicles would be unaltered with ageing.

2. Materials and methods

2.1. Sample collection and preparation

Forelimbs distal to the carpus were collected from half- to full-thoroughbred horses aged 3–6 years ($n = 12$, young group) and 17–20 years ($n = 12$, old group), euthanized at a commercial equine abattoir. Only tendons which had no evidence of previous tendon injury at post-mortem examination were included in the study. The SDFT and CDET were dissected free from the limbs from the level of the carpus to the metacarpophalangeal joint, wrapped in tissue paper dampened with phosphate buffered saline (PBS) and stored frozen at −20 °C wrapped in aluminium foil. It has previously been shown that one freeze–thaw cycle does not affect tendon mechanical properties [30]. On the day of testing, the tendons were allowed to thaw at room temperature and fascicles (~25 mm in length) were isolated by cutting with a scalpel longitudinally though the tendon using previously established protocols [31,32]. Fascicles were dissected from the core ($n = 3$ or 4 from each tendon) and periphery ($n = 3$ or 4 from each tendon) of the mid-metacarpal region of the SDFT and CDET. We have established that, while isolated fascicles show alterations in mechanical properties after freezing, there is no difference in the failure properties of fascicles dissected from fresh or frozen tendons (unpublished data). Fascicle hydration was maintained by storing the fascicles on tissue paper dampened with PBS. Fascicles were tested within a few hours of isolation to ensure that their structural integrity was maintained.

2.2. Mechanical testing protocols

2.2.1. Assessment of fibre level response to incrementally applied strain

Fascicles from the core and periphery of paired SDFTs and CDETs (6–8 fascicles) from a subset of four horses in the young age group were stained with the collagen stain 5-([4,6-dichlorotriazin-2-yl]amino)fluorescein hydrochloride (5-DTAF) at a concentration of 2 mg ml^{-1} in 0.1 M sodium bicarbonate buffer, pH 9 for 20 min. Following staining the fascicles were washed in two changes of PBS for 20 min, and secured in a custom-made tensile testing rig [28], at a resting length of 10 mm. Fascicles were maintained in PBS for the duration of the experiment. Initial experiments were performed to assess the effect of 5-DTAF on fascicle material properties (see Supplementary information).

Each fascicle was viewed under the laser scanning confocal microscope (TCS SP2, Leica Microsystems GmbH, Wetzlar, Germany) using a ×20 objective (HC PL Fluotar, Nikon, Kingston-Upon-Thames, UK). Fascicle alignment and orientation were checked under bright-field settings along the entire fascicle length to confirm that only single fascicles were tested. Any samples that showed evidence of gross torsion or damage were not tested. A tare load of ~0.1 N (range: 0.05–0.15 N) was applied. A grid was then photobleached onto the fascicle, using a 488 nm krypton–argon laser, encompassing a series of 2 μm thick lines, bleached in the central region of the fascicle, to create a grid of four squares, each 50 μm × 50 μm (Fig. 1a). The laser intensity was then reduced to the imaging range, and the sample imaged with the same objective lens at a resolution of 2048 × 2048 pixels, with each pixel measuring 0.18 × 0.18 μm. An image of the photobleached grid was taken in a focal plane ~20–25 μm from the sample surface. The fascicle was then strained to 2% at a rate of 1% s^{-1} and the grid was refocused, before imaging again (Fig. 1b and c). Incremental strains of 2% were applied up to a maximum of 10%, and the grid was imaged at each strain increment. There was a hold period of ~1 min before imaging at each increment, whilst the focal plane was located. Initial experiments were performed to ensure that overall applied strain was representative of mid-portion strains (see Supplementary information).

2.2.2. Determination of recoil capacity at fibre level

To assess the ability of the fascicles to recoil, a further 6–8 fascicles per tendon were taken from a subset ($n = 4$ paired SDFTs and CDETs) of the young tendon group. The fascicles were stained with

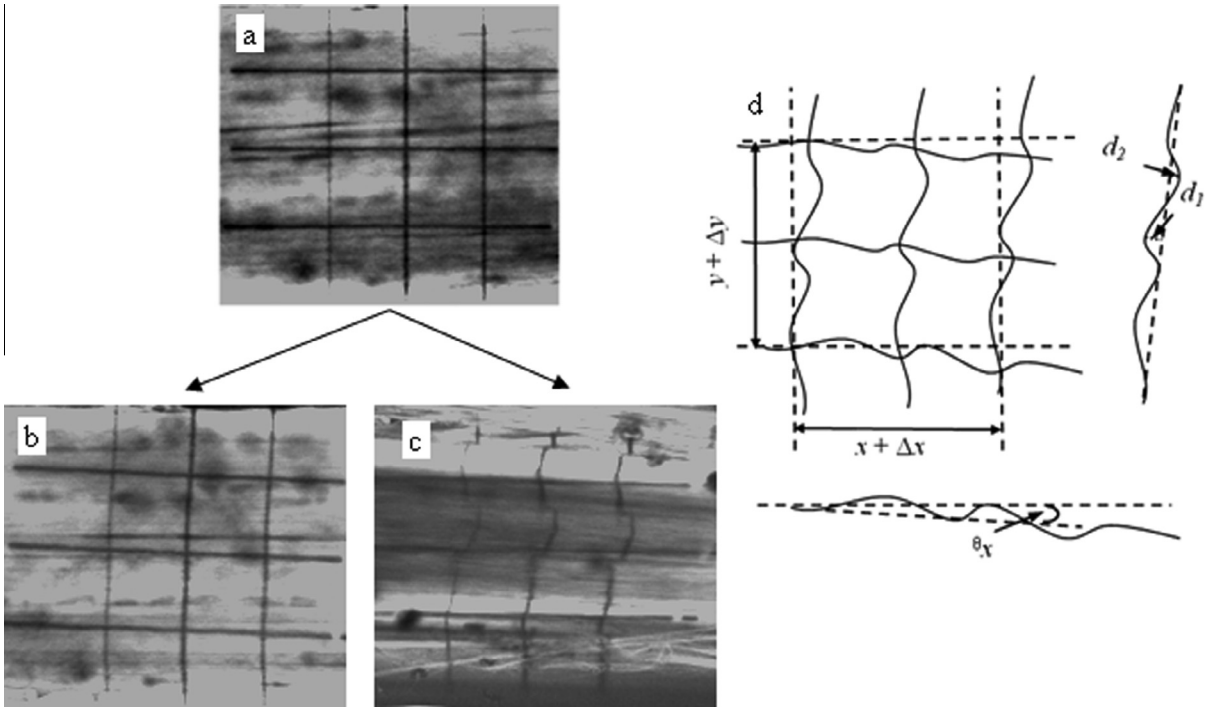

Fig. 1. Images showing grid bleached onto fascicles stained with 5-DTAF at 0% applied strain (a), and grid deformation at 4% applied strain in SDFT (b) and CDET (c) samples. Schematic (d) showing the four parameters used to quantify grid deformation.

5-DTAF and a grid bleached onto the samples as described above. A tare load of ~0.1 N was used to determine the start point of the test and the grid was imaged using the settings described above. A strain of 4% was then applied, and the grid was re-imaged. The sample was returned to the test start position and the grid re-imaged. This was repeated at a strain of 8% before once again returning to 0% strain and re-imaging. There was a hold time of ~1 min before imaging at each increment.

2.2.3. Determination of recoil capacity at fascicle level

To further investigate the efficacy of recoil, the extent of hysteresis loss was determined in SDFT and CDET fascicles. Fascicles from the core and periphery were dissected from a subset ($n = 4$ paired SDFTs and CDETs, 4–6 fascicles per tendon) of the young tendon group. Fascicle diameter was measured using a laser micrometer [11], and the resulting values used to calculate fascicle cross-sectional area (CSA), assuming a circular cross-section. Each fascicle was secured in a custom-made chamber system [32] at a resting length of 10 mm. Fascicles were maintained in PBS for the duration of the experiment. The chamber was secured in a materials testing machine (Bionix 100, MTS) and a tare load of 0.1 N was applied. In order to recapitulate the loading conditions from the confocal experiments described above, the sample was then strained to 4% and held at this strain for 1 min. The sample was returned to the test start point, and the test was repeated, taking the sample to 8% strain, with a hold period of 1 min before returning to 0% strain. Force–displacement data were collected at a rate of 50 Hz throughout the testing procedure. The resultant data were used to plot a stress–strain curve for each sample. From this, the percentage hysteresis loss was calculated for each recoil cycle at 4% and 8% strain (GraphPad Prism).

2.2.4. Effect of ageing on fibre and fascicle level mechanics

To study the effect of increasing age on the fibre and fascicle level mechanics in the SDFT and CDET, the incremental strain, recoil and hysteresis loss experiments described above were repeated on fascicles from tendons in the old group, using the same protocols and sample numbers as described above.

2.3. Image analysis

Images from the confocal experiments were processed using the analysis software Image J (1.34s, National Institute of Health, USA). The grid deformation parameters calculated are shown in Fig. 1d. In order to calculate the local x and y strains, the points where the lines in the x and y planes crossed were marked, and the image was thresholded and skeletonized; with the resulting image consisting of nine pixels representing the grid corners. The co-ordinates of these pixels were exported to Excel for data analysis. In order to quantify the local strains within the grid, the following parameters were calculated from the grid corner co-ordinates:

x strain ($100\Delta x/x$): Percentage strain in x direction (with axis of loading)
y strain ($100\Delta y/y$): Percentage strain in y direction (perpendicular to loading axis)

Poisson's ratios (v) were calculated at each strain increment using the following equation:

$$v = \frac{-y\ strain}{applied\ strain}$$

In order to calculate the maximum deviation of the vertical gridline (y axis), images were thresholded, despeckled and skeletonized in Image J to generate a single pixel trace of one of the lines in the y plane. Any noise was removed from the image and the co-ordinates of the line exported to Origin (OriginLab, Northampton, USA). A straight line was fitted between the start and end points of this line. The maximum deviations of the gridline from the straight line in both directions were also calculated ($d_1 + d_2$).

In order to quantify grid rotation, images were processed in Image J (as described above) to generate a single pixel trace of one of

the horizontal gridlines (x axis) and the co-ordinates of this line were exported to Origin. A linear line of best fit was fitted to the co-ordinates, and the angle of this line (θ_x) was calculated.

To assess the ability of the fascicle to recoil, the percentage recovery of each measure of grid displacement (local x and y strains, vertical gridline deviation and grid rotation) was calculated for each sample after 4% and 8% applied strain.

2.4. Statistical analysis

The distribution of the data was tested using a Kolmongorov–Smirnof test for normality. Data with a normal distribution were subjected to linear mixed effects analysis in SPlus. Data that were not normally distributed were tested using Wilcoxon rank-sum tests. Statistical significance was set at $p < 0.05$.

3. Results

3.1. Fibre response to applied strain

Images of the grids highlight large deformations within the fascicles at each strain increment. Further, it can be seen that the microstructural strain response differs between the functionally distinct SDFT and CDET (Fig. 1b and c). Quantification of grid deformations showed that there was no difference in the strain response of fascicles from the core or periphery of the tendon in either tendon type, so these data were combined for further analyses. It was not possible to obtain images of a high enough quality for analysis at 10% applied strain in sufficient CDET samples for statistical analysis, therefore data are shown up to 8% for SDFT and CDET comparisons (Fig. 2).

The data regarding local strains within the grids show that x strains, representing fibre extension, were much smaller than the overall applied strain (Fig. 2a), and did not differ significantly between the SDFT and CDET. In agreement with previous results [28], large y strains were observed perpendicular to the loading axis, particularly in the CDET. These strains exceeded the overall applied strains, and were significantly greater in the CDET than in the SDFT at all strain increments below 8% ($p \leqslant 0.027$; Fig. 2b). There was a linear relationship between applied strain and mean y strain in the SDFT, with a mean Poisson's ratio of 1.36 at all strain increments (Fig. 2c). By contrast, Poisson's ratios in the CDET exceeded those in the SDFT, but decreased with increasing strain increment. Therefore, Poisson's ratios were significantly greater in the CDET at and below 6% applied strain ($p \leqslant 0.027$, Fig. 2c).

Deviations of the vertical gridlines ($d_1 + d_2$) were observed in almost all samples, indicating that fibre sliding was occurring. Levels of fibre sliding were greater in the CDET than in the SDFT at all strain increments above 2% applied strain ($p \leqslant 0.006$; Fig. 2d). By contrast, the amount of grid rotation (θ_x) that occurred was significantly greater in the SDFT than in the CDET at all strain increments ($p \leqslant 0.032$; Fig. 2e).

3.2. Fascicle and fibre recovery response

The percentage recovery of x and y strain from 8% applied strain was significantly greater in SDFT fascicles than in CDET fascicles ($p \leqslant 0.03$; Fig. 3a and b). The recovery of fibre sliding was also significantly higher in the SDFT samples after both 4% and 8% applied strain ($p \leqslant 0.008$; Fig. 3c). After 4% applied strain, grid rotation in the SDFT returned to pre-strain levels, while the percentage recovery in the CDET was significantly less, only recovering an average of 20% ($p = 0.043$; Fig. 3d). After 8% applied strain, percentage recovery of rotation reached an average of 109% in the SDFT, once again showing a complete return to pre-load levels. It was not possible to measure the recovery of rotation in the CDET after 8% applied strain due to an insufficient number of images of a high enough quality for analysis.

Alongside the significantly greater recovery from loading in SDFT fascicles, the percentage of hysteresis loss was also significantly lower compared to CDET fascicles, both after 4% applied strain (25.3% in the SDFT vs. 53.5% in the CDET; $p < 0.001$; Fig. 4) and 8% applied strain (37.5% in the SDFT vs. 57.4% in the CDET; $p < 0.001$; Fig. 4).

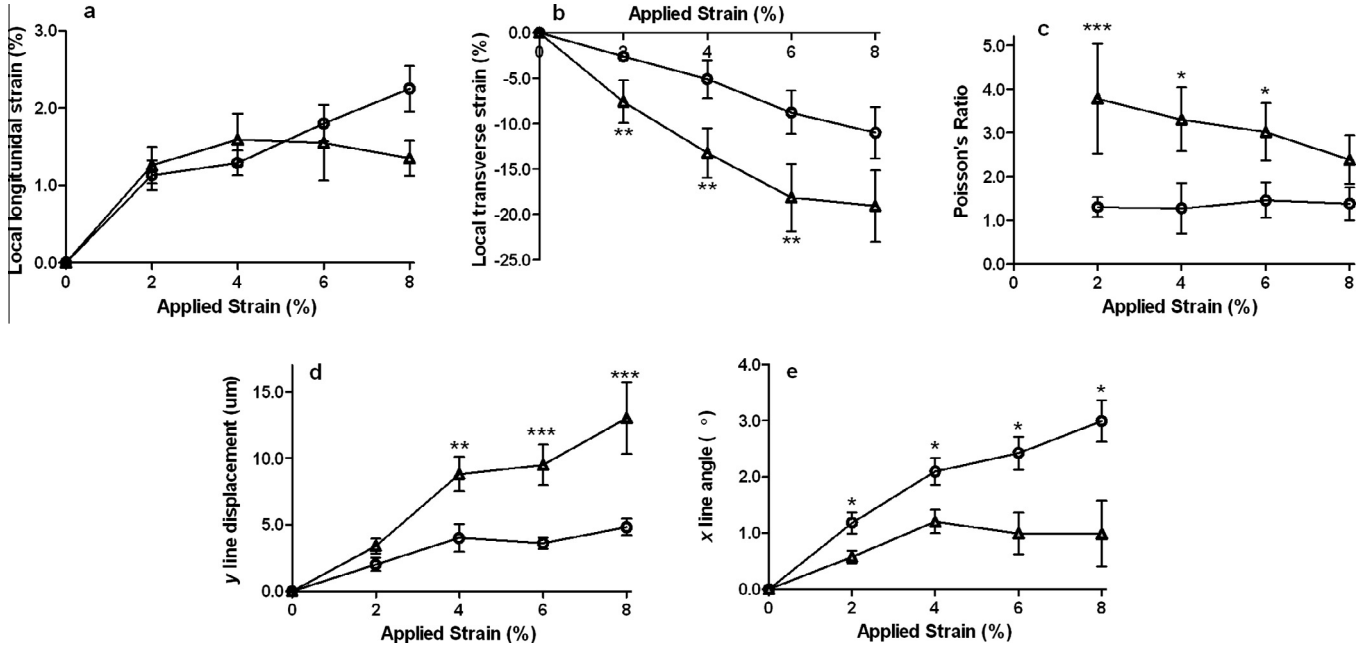

Fig. 2. Local longitudinal strains (a), transverse strains (b), Poisson's ratio (c) fibre sliding (d) and grid rotation (e) at increasing strain increments in the SDFT (○) and CDET (Δ). Data are displayed as mean ± SEM. Statistical significance: $^{*}p < 0.05$; $^{**}p < 0.01$; $^{***}p < 0.001$. It was not possible to obtain images of a high enough quality for analysis at 10% applied strain in sufficient CDET samples for statistical analysis, therefore data are shown up to 8% for SDFT and CDET comparisons.

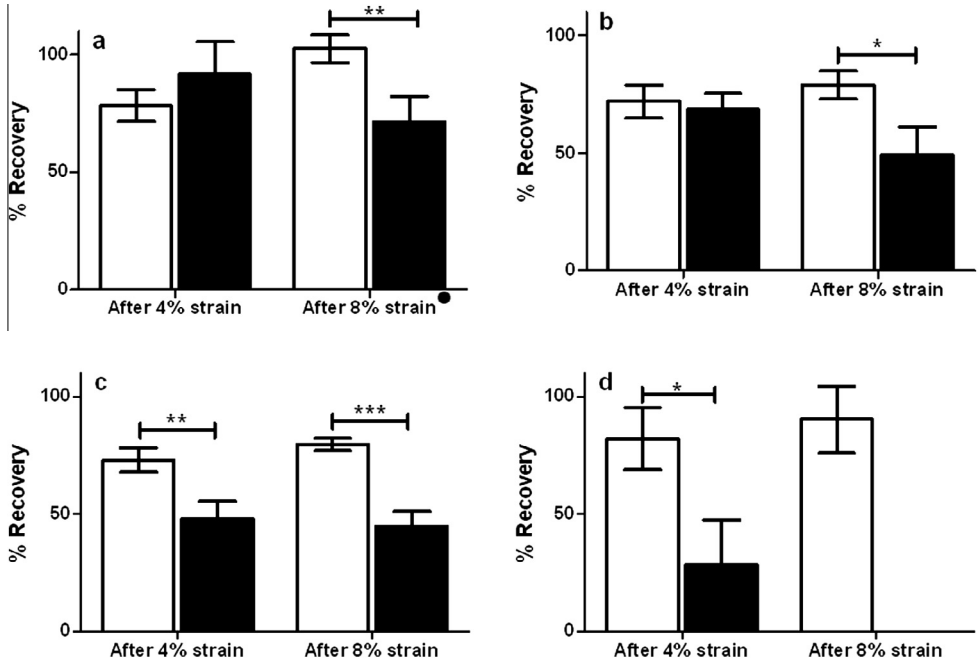

Fig. 3. Percentage recovery of *x* strain (a), *y* strain (b), *y* line displacement (c) and grid rotation (d) in the SDFT (□) and CDET (■) after the application of 4% and 8% strain. Data are displayed as mean ± SEM. Significance is indicated by: $^{*}p < 0.05$; $^{**}p < 0.01$; $^{***}p < 0.005$. It was not possible to measure the recovery of rotation in the CDET after 8% applied strain due to an insufficient number of images of a high enough quality for analysis.

3.3. Changes in fibre response to loading with increasing age

In the SDFT, there were several alterations in the fibre level response to applied strain in aged individuals. There was a decrease in transverse strain at all strain increments, with the exception of 8% applied strain ($p \leqslant 0.016$; Fig. 5a). This resulted in a significant decrease in Poisson's ratio below 8% applied strain ($p < 0.05$). There was also a decrease in grid rotation throughout loading, compared to samples from young horses; this became significant from 8% applied strain ($p \leqslant 0.033$; Fig. 5b). There were no age-related alterations in fibre level response to applied strain in CDET samples.

Age-related alterations in sample recovery after applied strain were also identified in the SDFT, with significantly reduced recovery of grid rotation after 8% applied strain ($p = 0.014$; Fig. 5c). Correspondingly, the percentage of hysteresis loss was significantly greater in aged SDFT samples, after 8% applied strain ($p < 0.048$; Fig. 5d). There were no age-related alterations in sample recovery or the percentage of hysteresis loss in CDET samples.

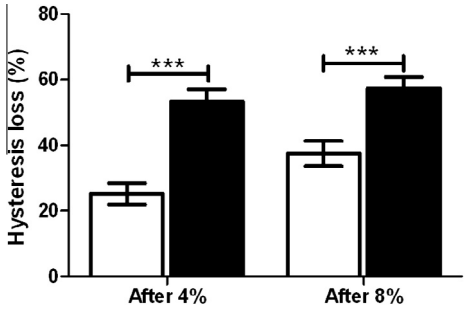

Fig. 4. Percentage hysteresis loss after 4% and 8% applied strain in the SDFT (□) and CDET (■). Data are displayed as mean ± SEM. Significance is indicated by: $^{***}p < 0.005$.

4. Discussion

The results of this study support our hypothesis that extension and recoil mechanisms differ in SDFT and CDET fascicles, leading to more efficient recoil in samples from the ES SDFT. This is the first study to document differences in the microstructural strain response in tendons with different functions, and directly associate these differences with the ability of fascicles to recoil after strain has been applied. In further support of the hypothesis, we have shown that age-related changes occur to the strain response of fascicles from the ES SDFT, and that these changes are associated with a decreased ability to recoil.

In agreement with previous studies on bovine extensor, and rat tail tendon fascicles [19,20,28,33], local longitudinal strains within the grid were consistently smaller than the overall applied strain in both tendon types, indicating that mechanisms other than fibre extension must contribute to overall fascicle extension. Previous studies have reported that extension in collagen-rich tissues is facilitated by high levels of sliding between adjacent fibres [25,28,29,34]. Further, it has been established that sliding occurs between collagen units at lower levels of the hierarchy, with second harmonic generation and X-ray diffraction studies showing sliding at the fibril scale [21,23,24]. The data in the current study support these previous findings, with some degree of fibre sliding observed in all samples. However, the current data also show that the typically reported fibre sliding is only prevalent in positional tendons, with sliding between adjacent fibres appearing to be the dominant mechanism facilitating overall extension in the CDET. By contrast, levels of fibre sliding were significantly lower in fascicles from the more extensible ES SDFT, indicating that additional mechanisms must enable fascicle extension in this tendon type. The majority of previous studies have used rat tail tendon fascicles as a simple model system for analysis. As rat tail tendon is clearly only positional, these results are not surprising and the current data highlight the need for care when using rat tail tendon fascicles to infer tendon response to loading, specifically when

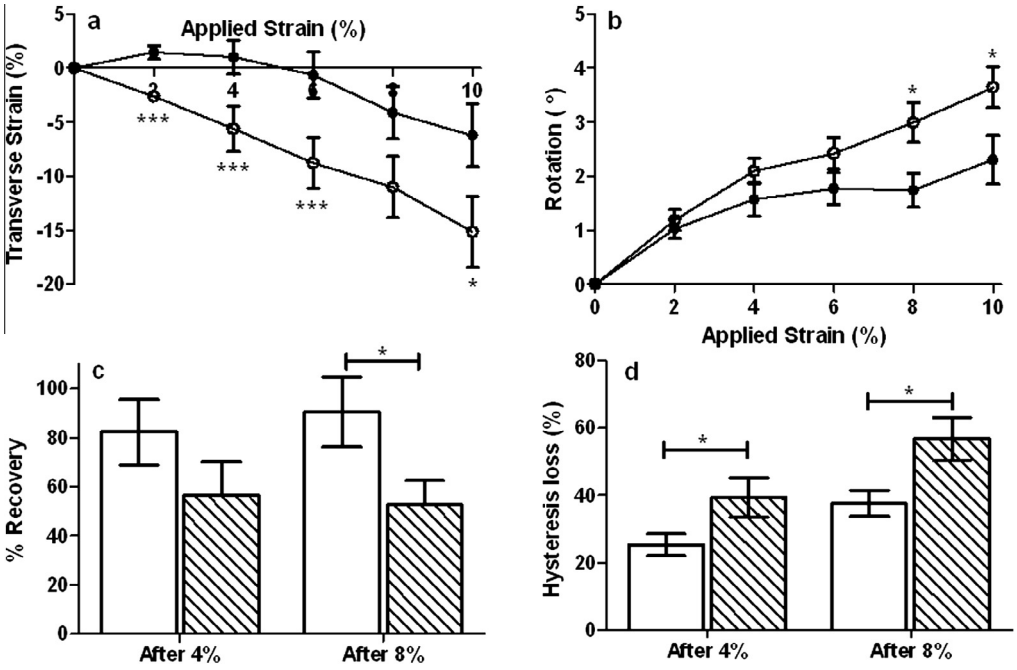

Fig. 5. Levels of transverse strain (a) and grid rotation (b) were greater in SDFT samples from young horses (○) than those from aged horses (●). Percentage recovery of rotation (c) was lower, and hysteresis loss (d) was greater in SDFT samples from aged horses (▨) compared to SDFT samples from young horses (□).

extrapolating data from this model system to the behaviour of ES tendons that are frequently affected by clinical injury.

Rotation of the grid was observed in almost all samples, supporting previous studies on rat tail tendon which report a small amount of rotation [28], suggesting that there may be a helical component to the fascicle structure. In previous work, fascicles have been described as frequently showing a spiral formation along the tendon length [35], and, more recently, microCT with three-dimensional (3-D) reconstruction has been used to demonstrate that fascicles within the human extensor carpi ulnaris tendon are arranged in a spiral at an angle of ∼8° to the longitudinal axis of the tendon [36].

It is well established that helices are present at lower levels of the tendon hierarchy, with right-handed triple helical collagen molecules forming the basis of the tendon structure [37]. The collagen molecules pack together to form helical right-handed microfibrils [38], which interdigitate with adjacent microfibrils to form left-handed helical fibrils [39]. There is also evidence to suggest the presence of a helix at the fibre and fascicle levels; microscopy studies have shown helical crimp patterns in bovine flexor tendon and rat tail tendon [40] as well as in canine patellar tendon and anterior cruciate ligament [41]. Interestingly, finite element modelling has shown that the presence of a helical superstructure within tendon predicts the extremely large Poisson's ratios observed in this study and by others [28,42], whereas the presence of planar crimp cannot account for the large compressive strains perpendicular to the loading axis [43]. These findings, combined with the grid rotations observed in the current study, strongly suggest the presence of a helix at the fascicle level.

Furthermore, the current study provides the first evidence of clear microstructural differences between tendon types, indicating that fibre helical rotation within the fascicle is less necessary for function in positional tendons. The greater rotation in the SDFT indicates that helix pitch angle may be greater in this ES tendon. In this tendon, extension may therefore be facilitated by straightening of the coil of the helix in addition to the small amount of fibre sliding observed. It may seem counterintuitive that larger Poisson's ratios were observed in the CDET, despite less rotation indicating a smaller helical pitch angle in this tendon type. However, it has been shown that the relationship between helical pitch angle and Poisson's ratio is complex, and is also affected by changes in crimp angle and the ratio of the fibre modulus to the matrix modulus [43]. As crimp angle increases, the resulting Poisson's ratio decreases [43]. It has been shown using rat tissue that crimp angle is greater in ES tendons than those with a positional function [44]. We have made measurements of crimp angle in equine SDFT and CDET (see Supplementary information) and found that the CDET has a significantly lower crimp angle than the SDFT. A smaller crimp angle in the positional CDET may therefore account for the larger Poisson's ratios in this tendon type. Interestingly, it has been suggested that crimp angle is directly related to elastic recoil capacity [45,46], and studies have shown a reduced crimp angle in aged tendons [47,48]; differences in crimp angle between tendon types may also contribute to the differences in recoil capacity reported in the current study.

Previous studies have also shown differences in helical appearances within and between tendinous structures. Yahia et al. [41] showed that all patellar tendon fascicles had a helical waveform but only those from the periphery of the anterior cruciate ligament showed this helical wave pattern, with central fascicles exhibiting a planar waveform. Further, Vidal and colleagues [40,49] have used birefringence to study crimp patterns in rat tail and Achilles tendons, and bovine flexor tendons, and report differences in birefringence distribution between tendons, which the authors suggest may indicate differences in the helical structure between species and/or tendon types [49]. Combined with the results from the present study, these previous data support the hypothesis that differences in helical structure between tendon types confer the specific and distinct mechanical properties required for efficient function.

However, the precise role of these helical components within tendon is not well understood. It has been suggested that the formation of a helix may confer greater stability [38] and the ability to resist rotational or multidirectional forces [28,36]; however, no

previous studies have directly linked a helix structure with the tendon loading response. The results of the current study show that the percentage recovery of all measures of grid displacement was significantly greater in SDFT samples, with significantly lower hysteresis loss than in the CDET. These results suggest that the helical component within fascicles may provide a mechanism to maximize recoil with minimal energy loss, a function which is crucial in high strain ES tendons. It is possible that a more tightly wound helix in ES tendons such as the equine SDFT and human Achilles would enable greater energy storage and return. Indeed, in some SDFT samples, recovery of rotation was greater than 100%; this may be as a result of the helix "springing" back. By contrast, in the positional CDET, the helix may be less tightly wound, as the capacity to extend and recoil significantly is not required under normal physiological loading, leading to poor recoil capacity in this tendon type. Indeed, these tendons require some viscoelasticity to modulate movement effectively; this may be facilitated by fibre sliding, which we have confirmed to be the predominant mechanism in relaxation mechanics in these positional tendons.

When interpreting the results, the levels of applied strain must be taken into consideration. While strains of 10% may appear high, our results show that, at a test length of 10 mm, fascicles fail at an average of 20% strain, and therefore a strain of 10% falls well within the linear region of the stress–strain curve for both tendon types. However, it is difficult to translate this information directly to the in vivo environment. The SDFT experiences significantly higher strains than the CDET during normal use [6,8], and correspondingly is able to extend further before failure when tested in vitro [10,11]. Conversely, previous work shows that SDFT fascicles fail at lower strains than those from the CDET, but there is the potential for a significant degree of sliding between fascicles in the SDFT, which is thought to enable the high strain characteristics of this tendon [11]. These results indicate that, while fascicles from the SDFT are likely to experience higher strains in vivo than those from the CDET, the differences are probably smaller than the differences in strain experienced by the whole tendons and therefore justify the approach taken in the present study to compare fascicles from the different tendons within the same range of strains.

In combination with these previous findings, the results of the current study strongly suggest that the distinct mechanical properties required by functionally different tendons are conferred by specializations in tendon structure at several hierarchical levels, as shown schematically in Fig. 6. It appears that the small amount of extension that occurs in the low strain positional CDET can be accommodated by sliding between adjacent fibres, with little or no fascicle sliding required [11]. By contrast, in the high strain ES SDFT, sliding between adjacent fascicles appears to allow initial tendon extension [11], while the presence of a helix may enable the fascicles to recoil more efficiently once they are loaded. However, the structure of this helix is as yet unclear, and further work is required to elucidate its precise structure and dimensions, as well as to identify specific differences between tendon types. This is of high importance as an improved understanding of how structures are specialized for their function, such as how ES tendons achieve greater elasticity, will not only allow us to better understand how different tissues function, but will also allow the development of more effective therapies and rehabilitation protocols.

When considering age-related alterations in the ability of fascicles to extend and recoil, the results show no age-related changes in any of the grid deformation parameters, percentage recovery or hysteresis loss in the CDET. However, we found that the microstructural strain response was altered with increasing age in the SDFT, with decreases in both transverse strain and rotation. A decrease in the helical pitch angle would account for both the reduction in rotation and smaller Poisson's ratios, as demonstrated by finite element analysis [43]. These changes are accompanied by a decrease in the percentage recovery of rotation, and increased hysteresis loss in aged SDFT samples. Taken together, these results suggest that there are age-related alterations to the helical component of fascicles from the ES SDFT, leading to a decreased ability to recoil efficiently. Previous work has shown that, while ageing does not result in changes to the ultimate properties of either the SDFT or the CDET, the capacity for sliding between adjacent fascicles

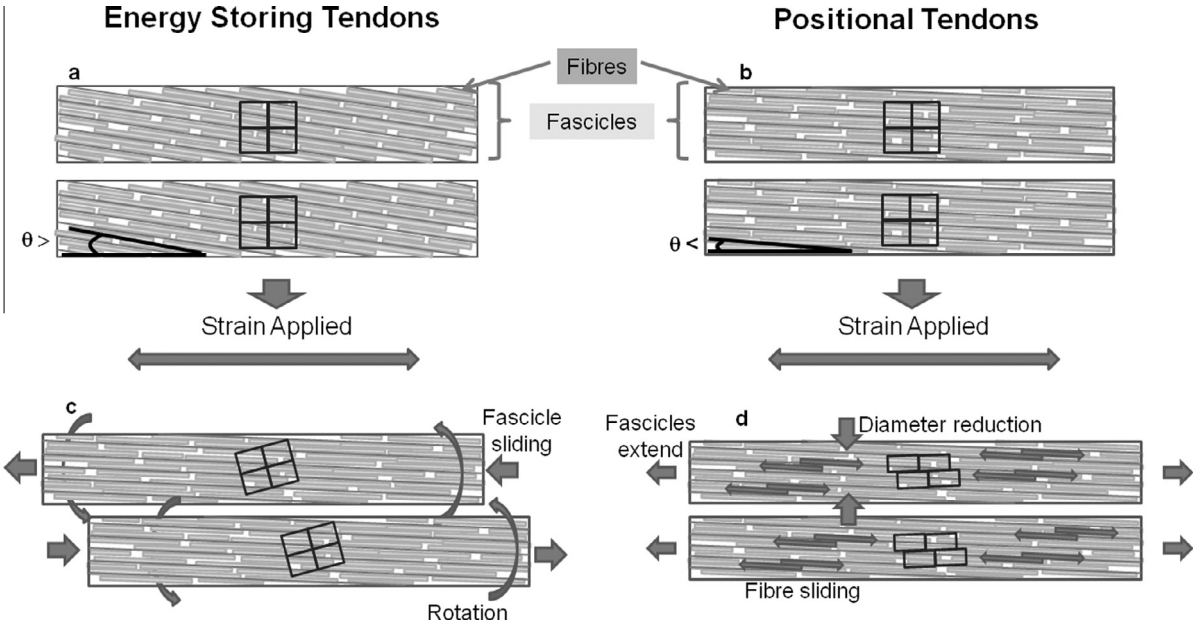

Fig. 6. Schematic illustrating differences in extension mechanisms between energy-storing and positional tendons. A greater helix pitch angle in fascicles within the ES SDFT (a) means that extension occurs due to unwinding of the helix, resulting in grid rotation (c). Further extension is facilitated by sliding between adjacent fascicles (c). By contrast, helical pitch angle is lower in the positional CDET (b); extension in this tendon type is governed by inter-fibre sliding, resulting in large deformations in the vertical gridlines (d), with little fascicle sliding (d).

decreases in aged SDFTs [50]. Further, it has been shown that partially degraded collagen accumulates in the SDFT, but not the CDET, from aged horses; this may lead to reduced mechanical competence [51]. All these changes are likely to decrease the fatigue resistance of the SDFT and may contribute to the increased risk of SDFT injury in aged individuals.

5. Conclusions

The current study highlights differences in extension and recoil mechanisms between functionally distinct tendons, and suggests the presence of a helix at the fascicle level. Further, the results suggest that differences in the helix structure between tendon types enables the greater recoil capacity observed in the ES SDFT, a function which is critical to maximize energy return. With increasing age, there appear to be alterations in the structure of the helix in the SDFT, resulting in less efficient recoil. This may decrease the fatigue resistance of aged SDFTs, and may be a factor predisposing aged tendons to overstrain injury.

Acknowledgements

This work was supported by a project Grant (prj/752) from the Horserace Betting Levy Board. We are grateful for the contribution of Miss Tracey Faram, who made the crimp angle measurements on equine tendon.

Appendix A. Supplementary data

Supplementary data associated with this article can be found, in the online version, at http://dx.doi.org/10.1016/j.actbio.2013.05.004.

References

[1] Kastelic J, Galeski A, Baer E. The multicomposite structure of tendon. Connect Tissue Res 1978;6:11–23.
[2] Alexander RM. Energy-saving mechanisms in walking and running. J Exp Biol 1991;160:55–69.
[3] Lichtwark GA, Wilson AM. Optimal muscle fascicle length and tendon stiffness for maximising gastrocnemius efficiency during human walking and running. J Theor Biol 2008;252:662–73.
[4] Lichtwark GA, Wilson AM. Is Achilles tendon compliance optimised for maximum muscle efficiency during locomotion? J Biomech 2007;40:1768–75.
[5] Roberts TJ, Azizi E. Flexible mechanisms: the diverse roles of biological springs in vertebrate movement. J Exp Biol 2011;214:353–61.
[6] Stephens PR, Nunamaker DM, Butterweck DM. Application of a Hall-effect transducer for measurement of tendon strains in horses. Am J Vet Res 1989;50:1089–95.
[7] Lichtwark GA, Wilson AM. In vivo mechanical properties of the human Achilles tendon during one-legged hopping. J Exp Biol 2005;208:4715–25.
[8] Birch HL. Tendon matrix composition and turnover in relation to functional requirements. Int J Exp Pathol 2007;88:241–8.
[9] Maganaris CN, Paul JP. In vivo human tendon mechanical properties. J Physiol 1999;521:307–13.
[10] Batson EL, Paramour RJ, Smith TJ, Birch HL, Patterson-Kane JC, Goodship AE. Are the material properties and matrix composition of equine flexor and extensor tendons determined by their functions? Equine Vet J 2003;35:314–8.
[11] Thorpe CT, Udeze CP, Birch HL, Clegg PD, Screen HRC. Specialization of tendon mechanical properties results from interfascicular differences. J R Soc Interface 2012;9:3108–17.
[12] Innes JF, Clegg P. Comparative rheumatology: what can be learnt from naturally occurring musculoskeletal disorders in domestic animals? Rheumatology (Oxford) 2010;49:1030–9.
[13] Lui PPY, Maffulli N, Rolf C, Smith RKW. What are the validated animal models for tendinopathy? Scand J Med Sci Sports 2010;21:3–17.
[14] Knobloch K, Yoon U, Vogt PM. Acute and overuse injuries correlated to hours of training in master running athletes. Foot Ankle Int 2008;29:671–6.
[15] Thorpe CT, Clegg PD, Birch HL. A review of tendon injury: why is the equine superficial digital flexor tendon most at risk? Equine Vet J 2010;42:174–80.
[16] Hess GW. Achilles tendon rupture: a review of etiology, population, anatomy, risk factors, and injury prevention. Foot Ankle Spec 2010;3:29–32.
[17] Perkins NR, Reid SWJ, Morris RS. Risk factors for injury to the superficial digital flexor tendon and suspensory apparatus in thoroughbred racehorses in New Zealand. N Z Vet J 2005;53:184–92.
[18] Kasashima Y, Takahashi T, Smith RK, Goodship AE, Kuwano A, Ueno T, et al. Prevalence of superficial digital flexor tendonitis and suspensory desmitis in Japanese Thoroughbred flat racehorses in 1999. Equine Vet J 2004;36:346–50.
[19] Screen HRC, Lee DA, Bader DL, Shelton JC. Development of a technique to determine strains in tendons using the cell nuclei. Biorheology 2003;40:361–8.
[20] Screen HRC, Bader DL, Lee DA, Shelton JC. Local strain measurement within tendon. Strain 2004;40:157–63.
[21] Gupta HS, Seto J, Krauss S, Boesecke P, Screen HRC. In situ multi-level analysis of viscoelastic deformation mechanisms in tendon collagen. J Struct Biol 2010;169:183–91.
[22] Screen HRC. Investigating load relaxation mechanics in tendon. J Mech Behav Biomed Mater 2008;1:51–8.
[23] Puxkandl R, Zizak I, Paris O, Keckes J, Tesch W, Bernstorff S, et al. Viscoelastic properties of collagen: synchrotron radiation investigations and structural model. Philos Trans R Soc Lond B Biol Sci 2002;357:191–7.
[24] Goulam Houssen Y, Gusachenko I, Schanne-Klein MC, Allain JM. Monitoring micrometer-scale collagen organization in rat-tail tendon upon mechanical strain using second harmonic microscopy. J Biomech 2011;44:2047–52.
[25] Snedeker JG, Pelled G, Zilberman Y, Gerhard F, Muller R, Gazit D. Endoscopic cellular microscopy for in vivo biomechanical assessment of tendon function. J Biomed Opt 2006;11:8.
[26] Snedeker JG, Pelled G, Zilberman Y, Ben Arav A, Huber E, Muller R, et al. An analytical model for elucidating tendon tissue structure and biomechanical function from in vivo cellular confocal microscopy images. Cells Tissues Organs 2009;190:111–9.
[27] Screen HRC, Toorani S, Shelton JC. Microstructural stress relaxation mechanics in functionally different tendons. Med Eng Phys 2012;35:96–102.
[28] Cheng VWT, Screen HRC. The micro-structural strain response of tendon. J Mater Sci 2007;42:8957–65.
[29] Bruehlmann SB, Matyas JR, Duncan NA. ISSLS prize winner: collagen fibril sliding governs cell mechanics in the anulus fibrosus. An in situ confocal microscopy study of bovine discs. Spine (Phila Pa 1976) 2004;29:2612–20.
[30] Huang H, Zhang J, Sun K, Zhang X, Tian S. Effects of repetitive multiple freeze–thaw cycles on the biomechanical properties of human flexor digitorum superficialis and flexor pollicis longus tendons. Clin Biomech 2011;26:419–23.
[31] Legerlotz K, Riley GP, Screen HR. Specimen dimensions influence the measurement of material properties in tendon fascicles. J Biomech 2010;43:2274–80.
[32] Legerlotz K, Jones GC, Screen HR, Riley GP. Cyclic loading of tendon fascicles using a novel fatigue loading system increases interleukin-6 expression by tenocytes. Scand J Med Sci Sports 2013;23:31–7.
[33] Arnoczky SP, Lavagnino M, Whallon JH, Hoonjan A. In situ cell nucleus deformation in tendons under tensile load; a morphological analysis using confocal laser microscopy. J Orthop Res 2002;20:29–35.
[34] Screen HRC, Lee DA, Bader DL, Shelton JC. An investigation into the effects of the hierarchical structure of tendon fascicles on micromechanical properties. Proc Inst Mech Eng H J Eng Med 2004;218:109–19.
[35] Kannus P. Structure of the tendon connective tissue. Scand J Med Sci Sports 2000;10:312–20.
[36] Kalson NS, Malone PS, Bradley RS, Withers PJ, Lees VC. Fibre bundles in the human extensor carpi ulnaris tendon are arranged in a spiral. J Hand Surg Eur Vol 2012;37:550–4.
[37] Silver FH, Freeman JW, Seehra GP. Collagen self-assembly and the development of tendon mechanical properties. J Biomech 2003;36:1529–53.
[38] Orgel JPRO, Irving TC, Miller A, Wess TJ. Microfibrillar structure of type I collagen in situ. Proc Natl Acad Sci USA 2006;103:9001–5.
[39] Franchi M, De Pasquale V, Martini D, Quaranta M, Macciocca M, Dionisi A, et al. Contribution of glycosaminoglycans to the microstructural integrity of fibrillar and fiber crimps in tendons and ligaments. ScientificWorldJournal 2010;10:1932–40.
[40] Vidal BdC. Image analysis of tendon helical superstructure using interference and polarized light microscopy. Micron 2003;34:423–32.
[41] Yahia LH, Drouin G. Microscopical investigation of canine anterior cruciate ligament and patellar tendon: collagen fascicle morphology and architecture. J Orthop Res 1989;7:243–51.
[42] Lynch HA, Johannessen W, Wu JP, Jawa A, Elliott DM. Effect of fiber orientation and strain rate on the nonlinear uniaxial tensile material properties of tendon. J Biomech Eng 2003;125:726–31.
[43] Reese SP, Maas SA, Weiss JA. Micromechanical models of helical superstructures in ligament and tendon fibers predict large Poisson's ratios. J Biomech 2010;43:1394–400.
[44] Franchi M, Quaranta M, Macciocca M, De Pasquale V, Ottani V, Ruggeri A. Structure relates to elastic recoil and functional role in quadriceps tendon and patellar ligament. Micron 2009;40:370–7.
[45] Franchi M, Fini M, Quaranta M, De Pasquale V, Raspanti M, Giavaresi G, et al. Crimp morphology in relaxed and stretched rat Achilles tendon. J Anat 2007;210:1–7.
[46] Benjamin M, Kaiser E, Milz S. Structure–function relationships in tendons: a review. J Anat 2008;212:211–28.

[47] Patterson-Kane JC, Firth EC, Goodship AE, Parry DA. Age-related differences in collagen crimp patterns in the superficial digital flexor tendon core region of untrained horses. Aust Vet J 1997;75:39–44.
[48] Diamant J, Keller A, Baer E, Litt M, Arridge RG. Collagen; ultrastructure and its relation to mechanical properties as a function of ageing. Proc R Soc Lond B Biol Sci 1972;180:293–315.
[49] Vidal BdC, Mello MLS. Optical anisotropy of collagen fibers of rat calcaneal tendons: an approach to spatially resolved supramolecular organization. Acta Histochem 2010;112:53–61.
[50] Thorpe CT, Udeze CP, Birch HL, Clegg PD, Screen HRC. Capacity for sliding between tendon fascicles decreases with ageing in injury prone equine tendons: a possible mechanism for age-related tendinopathy? Eur Cell Mater 2013;25:48–60.
[51] Thorpe CT, Streeter I, Pinchbeck GL, Goodship AE, Clegg PD, Birch HL. Aspartic acid racemization and collagen degradation markers reveal an accumulation of damage in tendon collagen that is enhanced with aging. J Biol Chem 2010;285:15674–81.